
SE 276B/MAE 232B: FINITE ELEMENTS IN SOLID MECHANICS

FINAL PROJECT REPORT

Name: Ru Xiang

Date: March 12th, 2019

1 Problem Statement

In this problem, we have an infinite long linear elastic tube with inner radius $R_i = 6\text{in}$, outer radius $R_o = 9.0\text{in}$, Young's modulus $E = 1000.0\text{psi}$, Poisson's ratio $\nu = 0.3$, density $\rho = 0.01\text{lb/in}^3$, which is subjected to a periodic ($T = 0.05\text{sec}$) internal pressure $P(t)$ on the internal surface:

$$P(t) = \begin{cases} \sin(\frac{2\pi t}{T}) & \text{for } 0 \leq t \leq \frac{T}{2} \\ 0 & \text{otherwise} \end{cases}$$

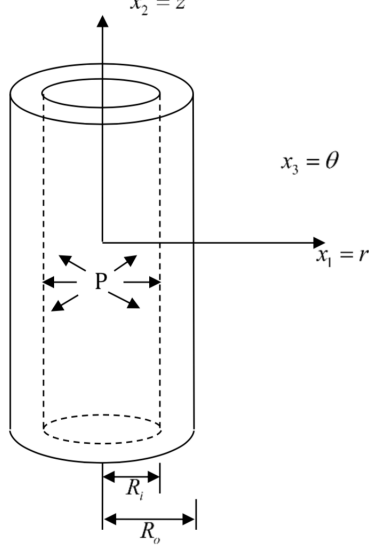


Figure 1: radial plane-strain problem.

To solve this problem, we used the following finite element formulations:

- Radial plane-strain: to reduce the 3D problem to 1D.
- Spatial discretization: 1 dimensional 2-node linear elements along the radial direction
- Temporal discretization: **Central difference method with lumped mass** and **Averaged acceleration method with consistent mass**.

2 Finite Element Formulation

2.1 Strong form

In 3D Cartesian coordinates, given E , ν , and ρ , find u such that,

$$\begin{aligned} \mathbf{B.C.s:} \quad & \sigma_{ij,j} + b_i = \rho \ddot{u}_i & \text{in} & \Omega \times]0, T[\\ & \sigma_{ij} r_j = -h & \text{on} & \Gamma^h \times]0, T[\\ \mathbf{I.C.s:} \quad & u(\bar{x}, t = 0) = 0. & \text{in} & \Omega \\ & \dot{u}(\bar{x}, t = 0) = 0. & \text{in} & \Omega \end{aligned}$$

2.2 Weak form

Find $u_i \in S \subset H^1$, such that, $\forall w_i \in V \subset H^1$, assuming zero body force,

$$\int_{\Omega} w_i (\rho \ddot{u}_i - \sigma_{ij,j}) d\Omega = 0$$

after derivation, we have

$$\underbrace{\int_{\Omega} w_i \rho \ddot{u}_i d\Omega}_1 + \underbrace{\int_{\Omega} w_{(i,j)} \sigma_{ij} d\Omega}_2 = \underbrace{\int_{\Gamma^h} w_i h_i d\Gamma}_3$$

For term 1, we reduce the integration from 3D to 1D by

$$\text{Term 1} = \int_{\Omega} w_i \rho \ddot{u}_i d\Omega = \int_0^h \int_0^{2\pi} \int_{R_i}^{R_o} \rho (w_r \ddot{u}_r + w_\theta \ddot{u}_\theta + w_z \ddot{u}_z) r dr d\theta dz = 2\pi h \int_{R_i}^{R_o} \rho w_r \ddot{u}_r r dr$$

$$\text{term 2} = \int_{\Omega} w_{(i,j)} \sigma_{ij} d\Omega = \int_{\Omega} w_{(i,j)} C_{ijkl} u_{kl,r} d\Omega$$

$$\text{Assume plane strain: } = \int_{\Omega} w_{(r,\theta)} \sigma_{rr} + w_{(\theta,\theta)} \sigma_{\theta\theta} + w_{(z,z)} \sigma_{zz} d\Omega$$

$$\epsilon_{22} = \epsilon_{12} = \epsilon_{13} = \epsilon_{23} = 0$$

Then the reduced constitutive relationship:

$$\Rightarrow \sigma_{12} = \sigma_{13} = \sigma_{23} = 0.$$

$$\begin{bmatrix} \sigma_{rr} \\ \sigma_{\theta\theta} \end{bmatrix} = \underbrace{\frac{E}{(1+\nu)(1-2\nu)} \begin{bmatrix} 1-\nu & \nu \\ \nu & 1-\nu \end{bmatrix}}_C \begin{bmatrix} \epsilon_{rr} \\ \epsilon_{\theta\theta} \end{bmatrix}$$

$$\text{term 3} = \int_{\Gamma^h} w_i h_i d\Gamma = \int_{\Gamma^h} w_r h_r d\Gamma$$

2.3 Galerkin approximation

$$(G) \quad u_r = u_r^h \in S^h \subset H^1$$

$$u_r \approx u_r^h$$

$$\ddot{u}_r \approx \ddot{u}_r^h$$

$$w_r \approx w_r^h$$

$$\int_{\Omega} w_i^h \rho \ddot{u}_i^h d\Omega + \int_{\Omega} w_{(i,j)}^h \sigma_{ij}^h d\Omega = \int_{\Gamma^h} w_i^h h_i d\Gamma$$

2.4 Finite element method

(M) Spatial discretization

$$\Omega = \bigcup_{e=1}^E \Omega^e, \text{ where } \Omega^I \cap \Omega^J = \emptyset, I \neq J$$

$$u_r^e = \sum_{i=1}^2 N_i d_i = \underline{N} \underline{d}^e \quad w_r^e = \sum_{i=1}^2 N_i c_i = \underline{N} \underline{c}^e$$

$$\dot{u}_r^e = \sum_{i=1}^2 N_i v_i = \underline{N} \underline{v}^e$$

$$\ddot{u}_r^e = \sum_{i=1}^2 N_i a_i = \underline{N} \underline{a}^e$$

$$\text{shape functions (linear 2-D)}$$

$$N = [N_1 \ N_2]$$

$$\underline{d}^e = [d_1 \ d_2]^T$$

$$\underline{v}^e = [v_1 \ v_2]^T$$

$$\underline{a}^e = [a_1 \ a_2]^T$$

$$N_1(\xi) = \frac{1}{2}(1-\xi)$$

$$N_2(\xi) = \frac{1}{2}(1+\xi)$$

$$r(\xi) = N_1 r_1^e + N_2 r_2^e$$

$$\frac{\partial r(\xi)}{\partial \xi} = \frac{r_2^e - r_1^e}{2} = \frac{l_e}{2}$$

$$\frac{\partial N_1}{\partial \xi} = \frac{\partial N_1}{\partial r} \cdot \frac{\partial r}{\partial \xi} = (-\frac{1}{2})(\frac{2}{l_e}) = -\frac{1}{l_e}$$

$$\frac{\partial N_2}{\partial \xi} = \frac{1}{l_e}$$

term 1 = $2\pi h \int_{R_i}^{R_o} p w_r^e \dot{u}_r^e h dr$

$$= 2\pi h \sum_{e=1}^{NEL} \int_{r_e}^{r_o} p w_r^e \dot{u}_r^e r dr$$

$$= \sum_{e=1}^{NEL} (\underline{c}^{eT}) \underbrace{\left[2\pi h \int_{r_e}^{r_o} p N^T \underline{N} r dr \right]}_{\triangleq M^e} \underline{a}^e$$

$$M^e = 2\pi h \int_{r_e}^{r_o} p N^T \underline{N} r dr = 2\pi h \int_{-1}^1 p N^T(\xi) \underline{N}(\xi) r(\xi) \frac{dr}{d\xi} d\xi$$

$$= 2\pi h \sum_{j=1}^{NNT} p N^T(\xi_j) \underline{N}(\xi_j) r(\xi_j) \frac{dr}{d\xi} \Big|_{\xi=\xi_j} w_j.$$

Strain approximation

$$\begin{bmatrix} \epsilon_{rr} \\ \epsilon_{\theta\theta} \\ u_r^e \end{bmatrix} = \begin{bmatrix} \frac{\partial u_r^e}{\partial r} \\ \frac{u_r^e}{r} \end{bmatrix} = \begin{bmatrix} \sum_{i=1}^2 \frac{\partial N_i}{\partial r} d_i^e \\ \sum_{i=1}^2 N_i d_i^e \end{bmatrix} = \underbrace{\begin{bmatrix} \frac{\partial N_1}{\partial r} & \frac{\partial N_2}{\partial r} \\ \frac{N_1}{r} & \frac{N_2}{r} \end{bmatrix}}_{\triangleq B} \begin{bmatrix} d_1^e \\ d_2^e \end{bmatrix} = \underline{B} \underline{d}^e$$

For element m ,

$$\underline{B} = \begin{bmatrix} -\frac{1}{l_e} & \frac{1}{l_e} \\ \frac{1-\xi}{2r(\xi)} & \frac{1+\xi}{2r(\xi)} \end{bmatrix}$$

Stiffness matrix:

$$\text{term 2} = \int_{\Omega} w_r^k \delta_{ij}^k dr = \int_{\Omega} \left[\frac{\partial w_r^k}{\partial r} - \frac{w_r^k}{r} \right] \delta_{ij}^k \left[\frac{\partial u_r^k}{\partial r} \right] dr \\ = \sum_{e=1}^{N_{EL}} (C_e^T) \underbrace{\left[2\pi h \int_{\Omega_e} B_e^T C_e B_e dr \right]}_{\triangleq K_e^e} d^e$$

$$K_e^e = 2\pi h \int_{-1}^{+1} B_e^T C_e B_e r(z_j) \frac{dr(z_j)}{dz} dz$$

$$= 2\pi h \sum_{j=1}^{N_{ENR}} B_e^T(z_j) \int_{-1}^{+1} B_e(z_j) r(z_j) \frac{dr(z_j)}{dz} \Big|_{z=z_j} \cdot w_j$$

$$\text{term 3} = \int_{\Gamma^k \cap \Gamma^e} w_r^k h n \cdot d\Gamma = \sum_{e=1}^{N_{EL}} (C_e^T) \underbrace{\left[2\pi h \int_{\Gamma^k \cap \Gamma^e} N^T h n \cdot d\Gamma \right]}_{\triangleq f_e^e}$$

$$f_e^e = \begin{cases} 2\pi R_i h \begin{bmatrix} P(t) \\ 0 \end{bmatrix} & \text{if } m=1 \\ \begin{bmatrix} 0 \\ 0 \end{bmatrix} & , \text{ otherwise} \end{cases}$$

Then the problem is reduced to the semi-discrete equation:

$$\mathbf{M}\mathbf{d}(t) + \mathbf{K}\mathbf{d}(t) = \mathbf{f}(t). \quad (1)$$

3 Numerical Approach: Newmark method

By temporal discretization, let

$$\mathbf{d}_{n+1} \approx \mathbf{d}(t_{n+1})$$

$$\mathbf{v}_{n+1} \approx \mathbf{v}(t_{n+1})$$

$$\mathbf{a}_{n+1} \approx \mathbf{a}(t_{n+1}).$$

Then we have the full discrete equation:

$$\mathbf{M}\mathbf{a}_{n+1} + \mathbf{K}\mathbf{d}_{n+1} = \mathbf{f}_{n+1}. \quad (2)$$

For each time step, we first calculate the **predictors**,

$$\tilde{\mathbf{d}}_{n+1} = \mathbf{d}_n + \Delta t \mathbf{v}_n + \frac{1}{2}(1-2\beta)\Delta t^2 \mathbf{a}_n.$$

$$\tilde{\mathbf{v}}_{n+1} = \mathbf{v}_n + (1-\gamma)\Delta t \mathbf{a}_n.$$

And then obtain the solution for \mathbf{a}_{n+1} by

$$\mathbf{M}^* \mathbf{a}_{n+1} = \mathbf{f}_{n+1}^*$$

where

$$\mathbf{M}^* = \mathbf{M} + \beta \Delta t^2 \mathbf{K}$$

$$\mathbf{f}_{n+1}^* = \mathbf{f}_{n+1} - \mathbf{K}\tilde{\mathbf{d}}_{n+1}.$$

Finally we calculate the **correctors** for the next time step,

$$\mathbf{d}_{n+1} = \tilde{\mathbf{d}}_{n+1} + \beta \Delta t^2 \mathbf{a}_{n+1}.$$

$$\mathbf{v}_{n+1} = \tilde{\mathbf{v}}_{n+1} + \gamma \Delta t \mathbf{a}_{n+1}.$$

4 Numerical analysis

For the class project, we studied two types of Newmark methods, central difference with lumped mass and averaged acceleration with consistent mass, different by the choices of β and γ . And we also evaluated the stability of the two approaches regarding their constraints to the time step sizes and the performance of accuracy. Here are the study processes.

Table 1: Methods for time integration

Method	β	γ	Stability
Central difference method with lumped mass	0	$\frac{1}{2}$	conditionally stable with $\Delta t_{cr} = \frac{2}{\sqrt{\lambda_{max}}}$
Averaged acceleration method with consistent mass	$\frac{1}{4}$	$\frac{1}{2}$	unconditionally stable

4.1 Theoretical expectations

By mathematical stability analysis, which we have derived in the lecture or homework, the central difference method is conditionally stable with the critical time step size

$$\Delta t_{cr} = \frac{2}{\sqrt{\lambda_{max}}},$$

where λ_{max} is the largest eigenvalue of $\mathbf{M}^{-1}\mathbf{K}$. As for averaged acceleration method, it is unconditionally stable regardless of the time step size.

4.2 Numerical results

First we need to show that both of two algorithms works well with proper value of time step size and element refinement. And we choose three study points to be on. Here we can observe from Fig.2 that when $n_{ele} = 81$, $\Delta t = 0.8 \times \Delta t_{cr}$, both of the two methods can get smooth estimation of results as expected (for this case, $\Delta t_{cr} = 1.0095 \times 10^{-4}$ sec). And in the following sections we can analyze the stability of the methods when varying the algorithm parameters.

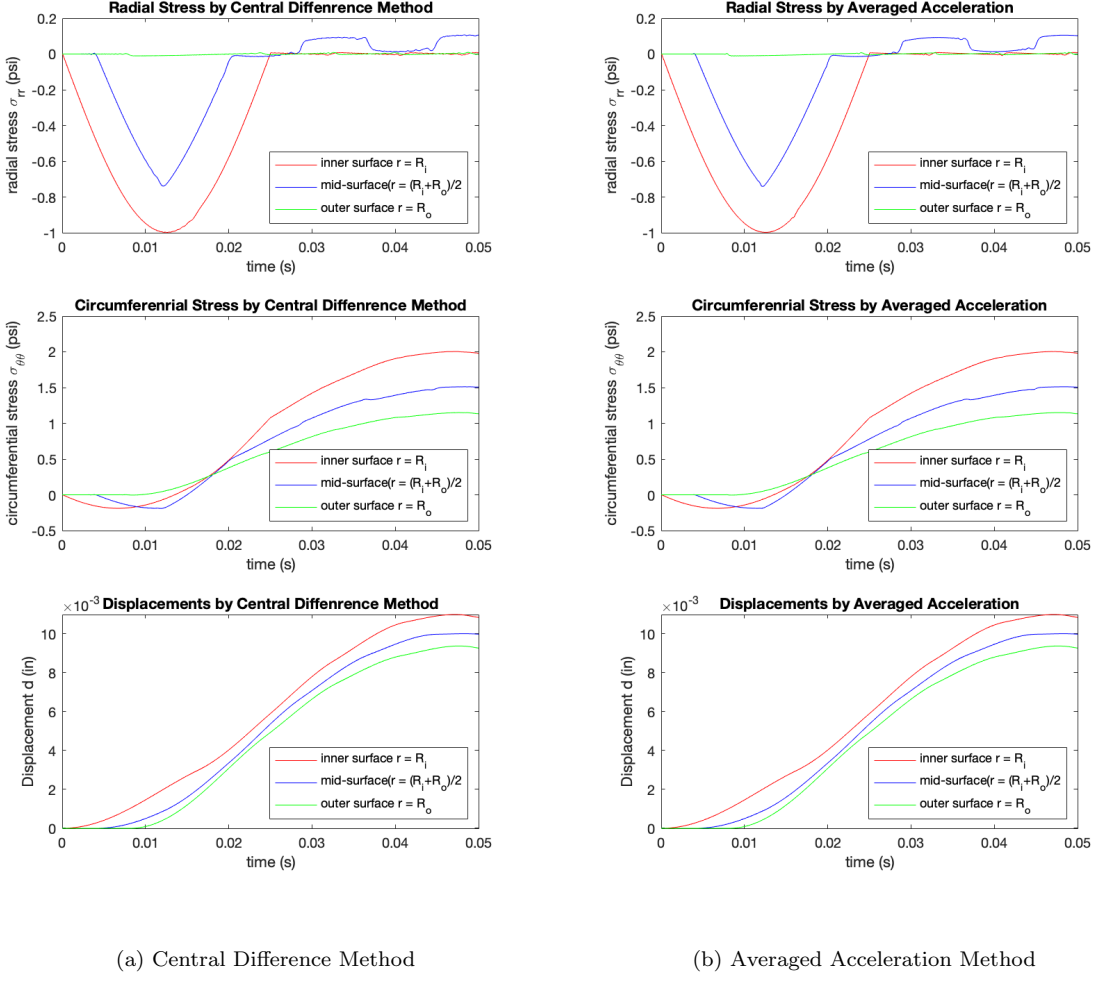


Figure 2: Numerical results when $n_{ele} = 81$, $\Delta t = 0.8 \times \Delta t_{cr}$

4.3 Stability of the two temporal discretization approaches

For this part of stability analysis, we set the number of spatial step size fixed with number of element $n_{ele} = 81$. And then compare the performance of stability of the two methods under the same time step sizes.

First we set the time step size $\Delta t = 1.0 \times \Delta t_{cr}$ for central difference, where the Δt_{cr} was obtained under $n_{ele} = 81$ with lumped mass. And then we tested the averaged acceleration method under the same time step size.

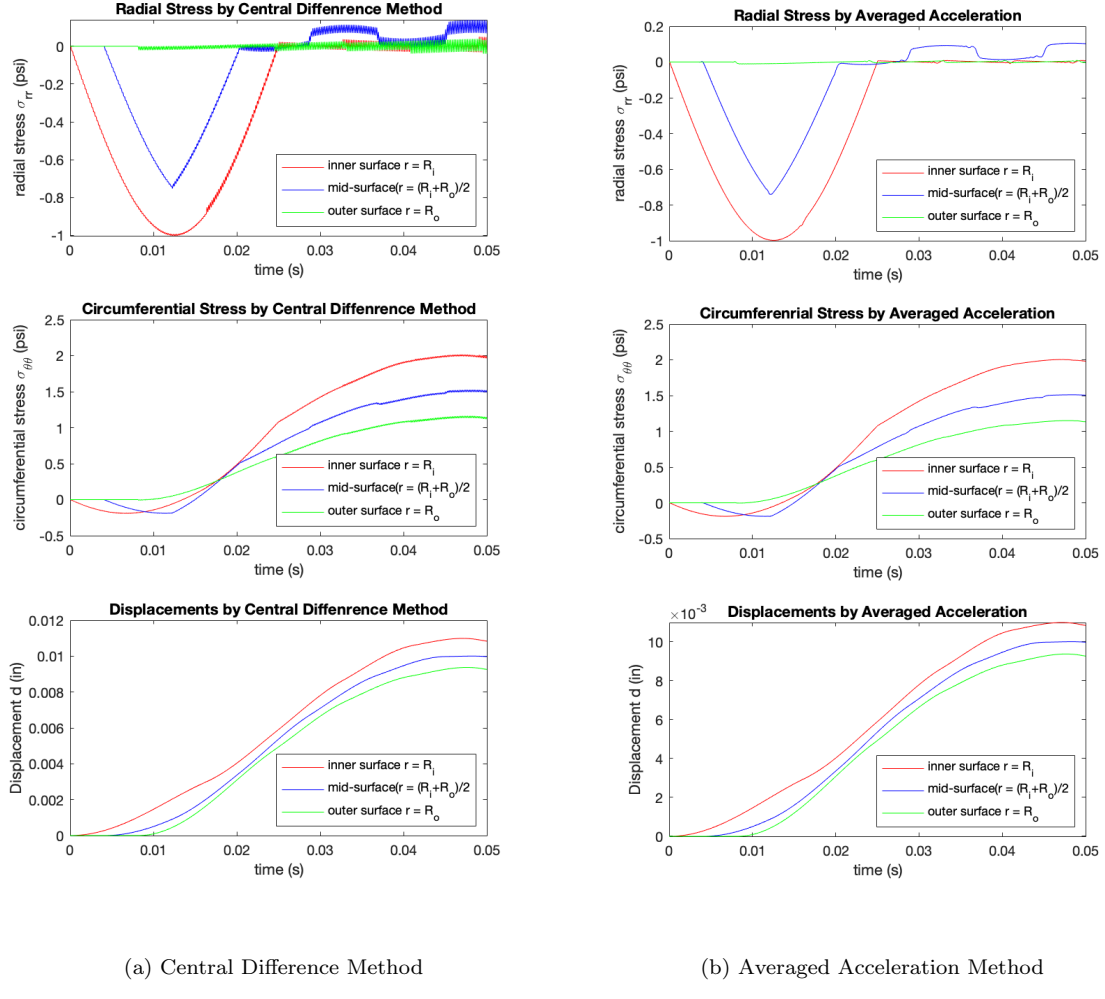


Figure 3: Numerical results when $n_{ele} = 81$, $\Delta t = 1.0 \times \Delta t_{cr}$

In Fig.3(a), the results of radial stress by central difference method became noisy and oscillated greatly. Also, there were small noises in results of circumferential stress and displacements. However, the results by averaged acceleration shown in Fig.3(b) were as stable as the results in Fig.2(b) when time step size is $0.8\Delta t_{cr}$. Hence we can conclude that the averaged acceleration method with consistent mass is more stable than the central difference method with lumped mass.

4.4 The effect of time step size on the stability

4.4.1 Central Difference Method

For Central Difference Method, we set the time step size to be 0.8, 1.0 and 1.2 times the critical time step size and observed their performance.

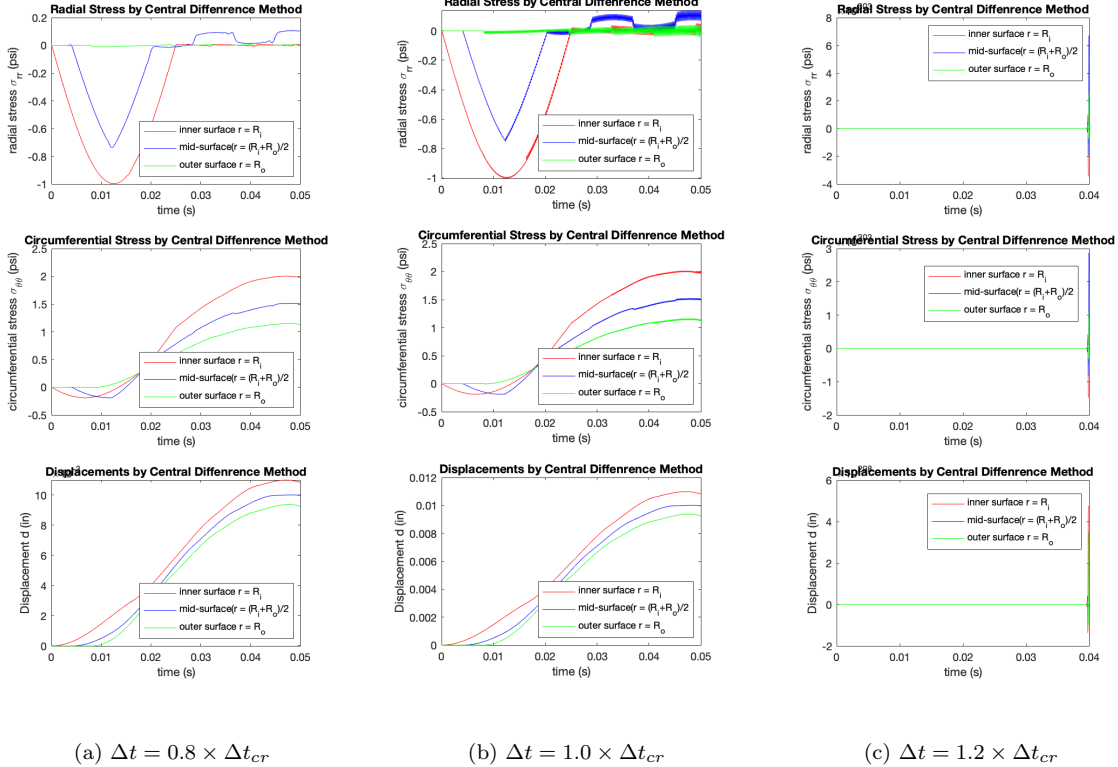


Figure 4: Numerical results by Central Difference Method of different time step sizes when $n_{ele} = 81$

From Fig.4, we found that the algorithm was stable for $\Delta t = 0.8 \times \Delta t_{cr}$, but became noisy when $\Delta t = 1.0 \times \Delta t_{cr}$ and even failed when $\Delta t = 1.2 \times \Delta t_{cr}$. Hence the method is restricted by the time step size and only achieves stability when Δt is small enough.

4.4.2 Averaged Acceleration Method

For Averaged Acceleration Method, we set the time step size to be 10^{-5} , 10^{-4} and 10^{-3} secs, the last one of which is much larger than the critical time step size in Central Difference Method.

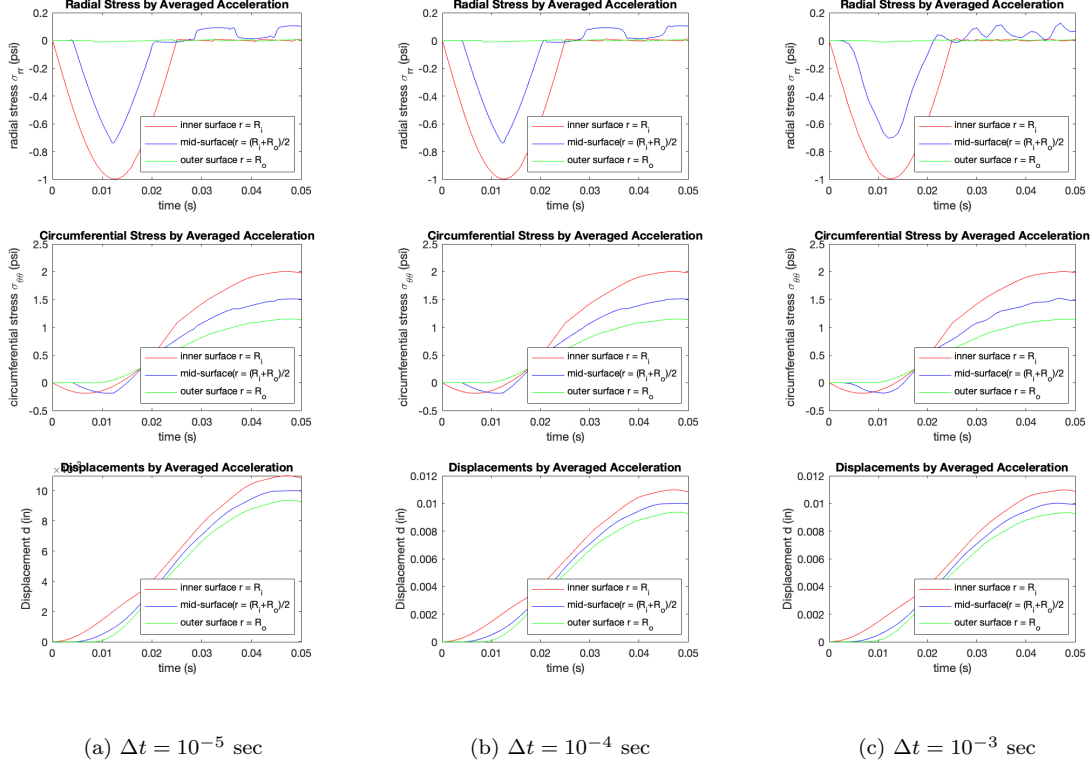


Figure 5: Numerical results by Averaged Acceleration Method of different time step sizes when $n_{ele} = 81$

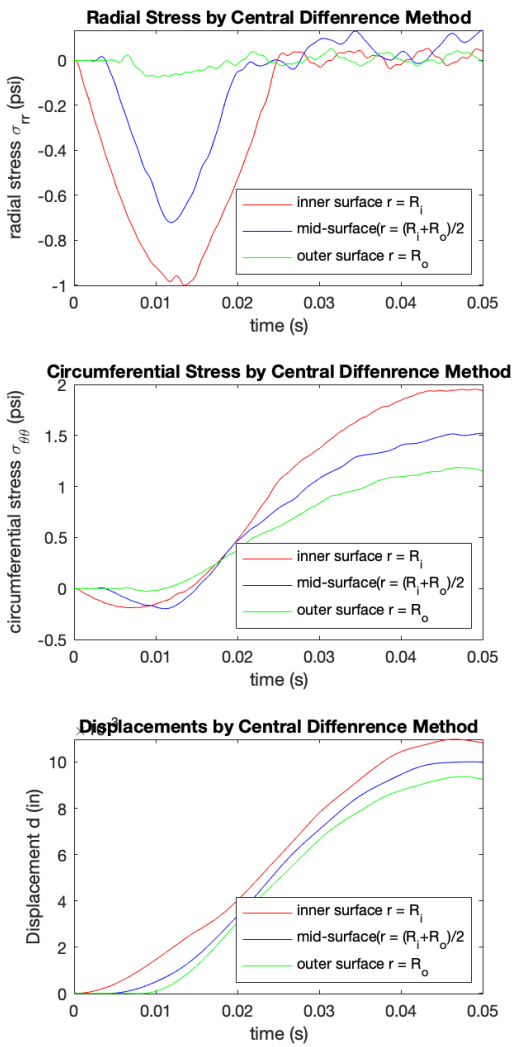
From Fig.5, we can see that in all the three conditions, the algorithm was always stable, while the values of numerical results were not exactly the same. Then we can conclude that the time step size would not affect the stability of the Averaged Acceleration Method.

4.5 The effect of element refinement on the accuracy

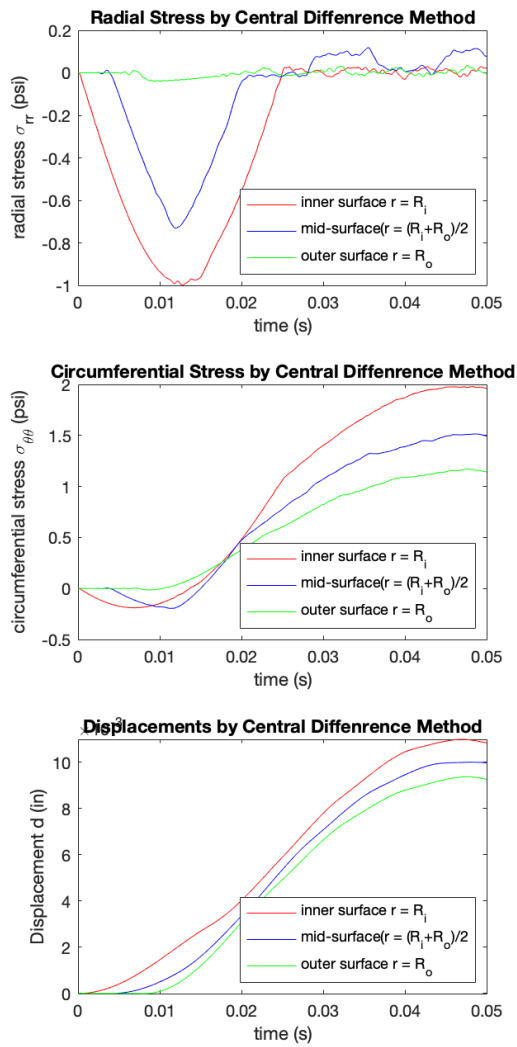
To study the effect of element refinement of accuracy, we should have the time step size fixed at 10^{-5} sec, which can promise the stability of both methods, and then calculating the norm of errors with 11, 21, 41, and 81 elements for spatial discretization.

4.5.1 Time history with different number of elements

By doing the same plot for each choice of number of elements, we found the most obvious difference existing in the radial stress plot, that the curve became smoother as we increased the number of elements from 11 to 81. This observation holds for both Central Difference Method (Fig.6) and Averaged Acceleration Method (Fig.7).



(a) $n_{ele} = 11$



(b) $n_{ele} = 21$

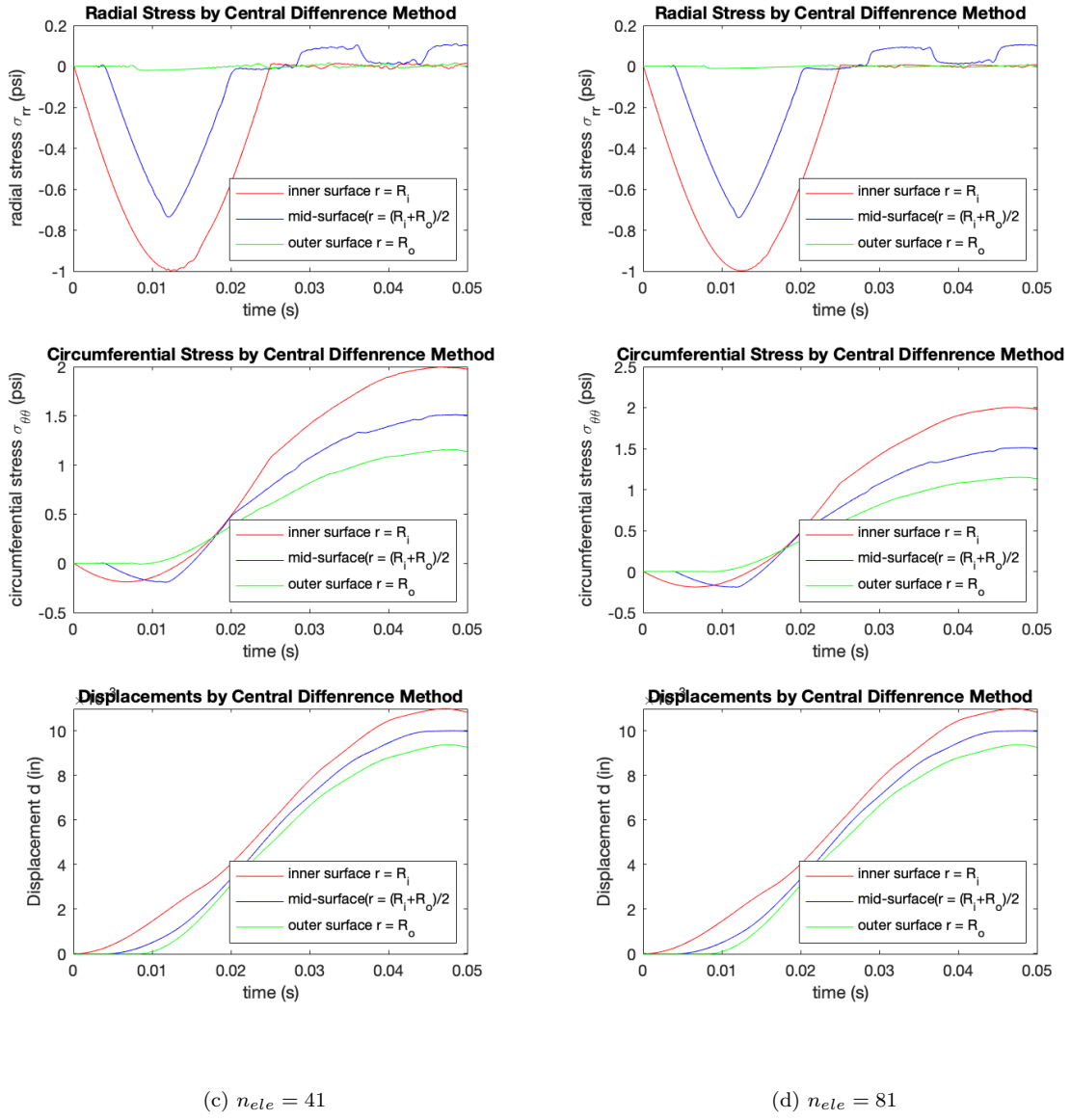
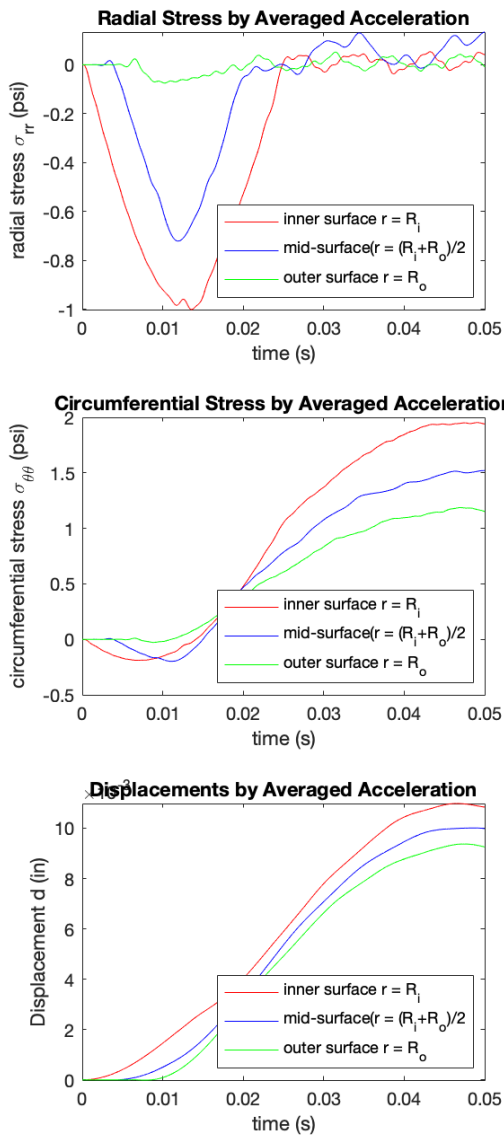
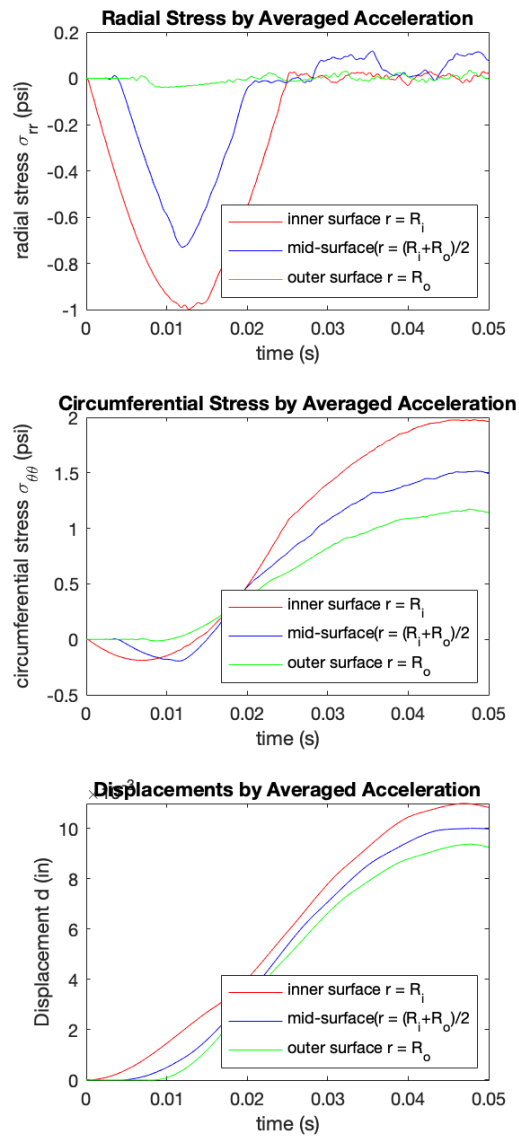


Figure 6: Numerical results by Central Difference Method with different number of elements when $\Delta t = 10^{-5}$ sec



(a) $n_{ele} = 11$



(b) $n_{ele} = 21$

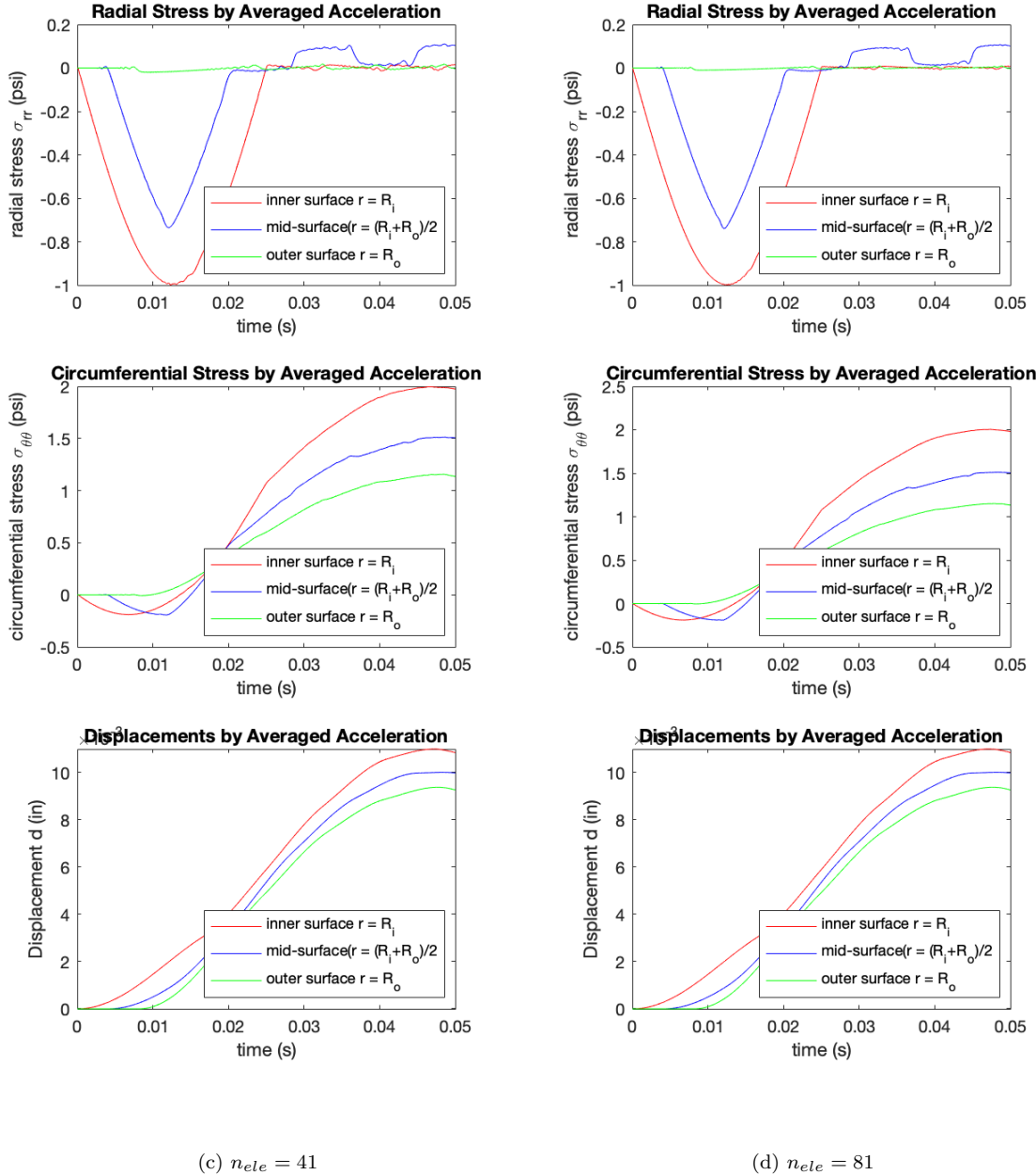
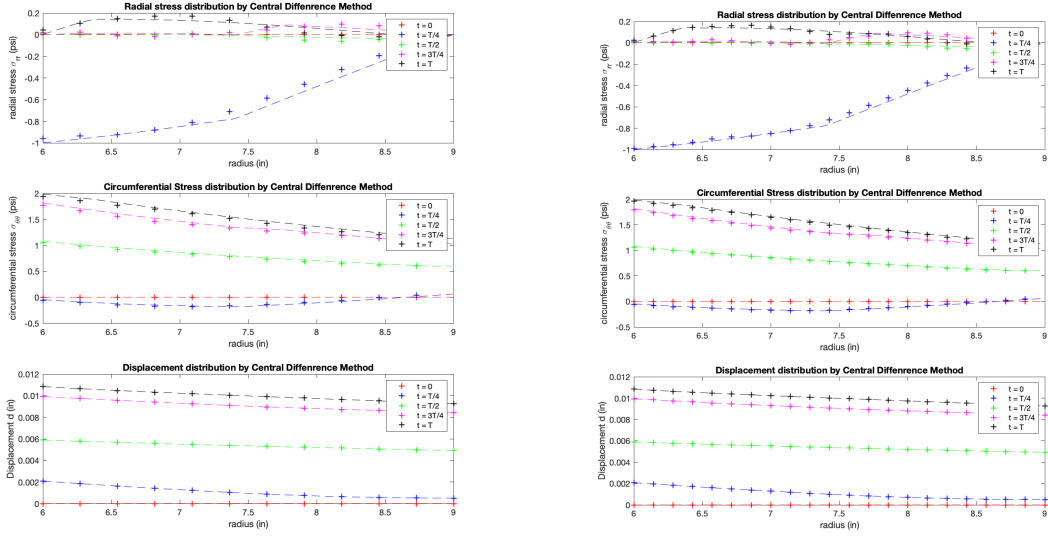


Figure 7: Numerical results by Averaged Acceleration Method with different number of elements when $\Delta t = 10^{-5}$ sec.

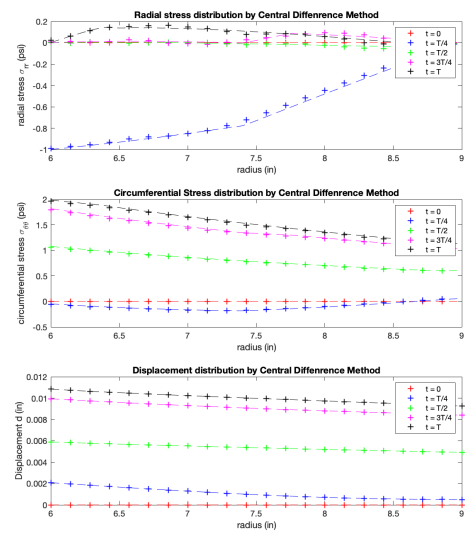
4.5.2 Displacement and stress distribution along the radius direction

Use the 401-element refinement as the reference, (dash line in each plot), we can study the error between the FEM results compared to analytical results (401-element) for different number of elements.

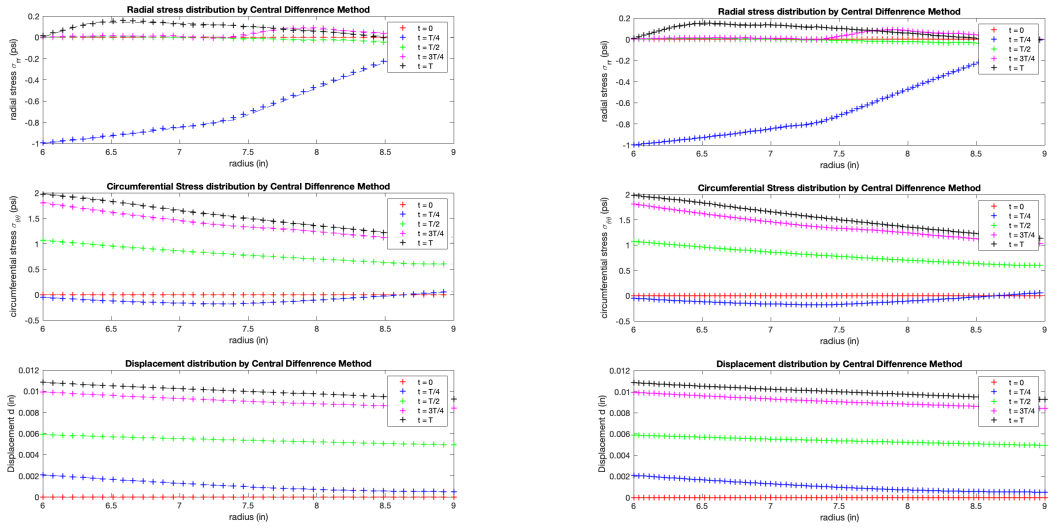
To see the performance at different time, we chose the numerical results record at $t = 0, \frac{T}{4}, \frac{T}{2}, \frac{3T}{4}$, and T .



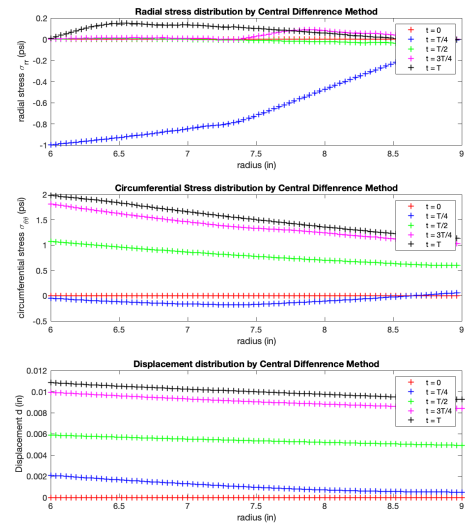
(a) $n_{ele} = 11$



(b) $n_{ele} = 21$

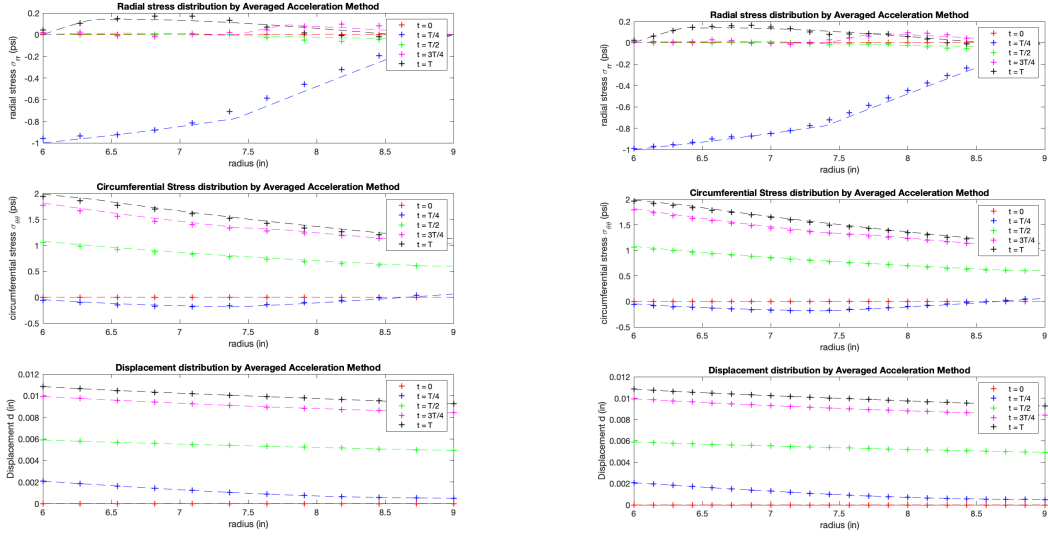


(c) $n_{ele} = 41$



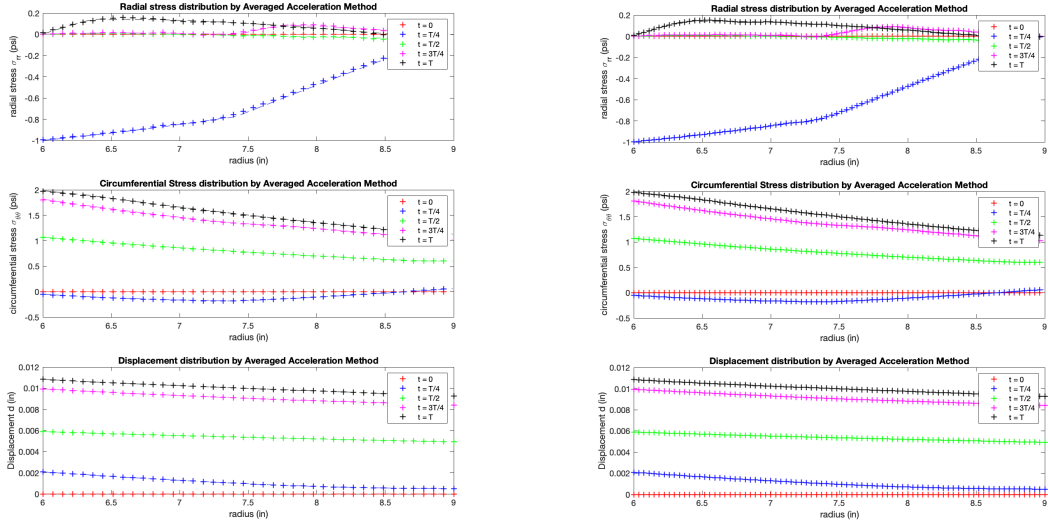
(d) $n_{ele} = 81$

Figure 8: Numerical results by Central Difference Method with different number of elements when $\Delta t = 10^{-5}$ sec.



(a) $n_{ele} = 11$

(b) $n_{ele} = 21$



(c) $n_{ele} = 41$

(d) $n_{ele} = 81$

Figure 9: Numerical results by Averaged Acceleration Method with different number of elements when $\Delta t = 10^{-5}$ sec.

For both methods, we can have the same observations:

- For nodal displacements, the results are accurate for 11, 21, 41, and 81 elements, compared to the 401-element reference values.
- For radial and circumferential stresses, it is clear to see how the results are approaching the analytical results when we increase the number of elements. For example, the error of radial stress results in Fig.7/8(a) with 11 elements are much larger than the error of radial stress in Fig.7/8(d) with 81 elements.

- Even for different time, the estimation of accuracy is the same, that the results are more accurate with more elements.

Moreover, by theoretical analysis, for linear element, the convergence rate of error in displacements should be 2, though not calculated specifically in this report.

4.6 Further study on the matched methods

With fixed number of elements $n_{ele} = 81$ and time step size $\Delta t = 10^{-5}$ sec, we can set the time to end to be $T_{end} = 0.4$ sec and observe the periodic oscillation of the numerical results.

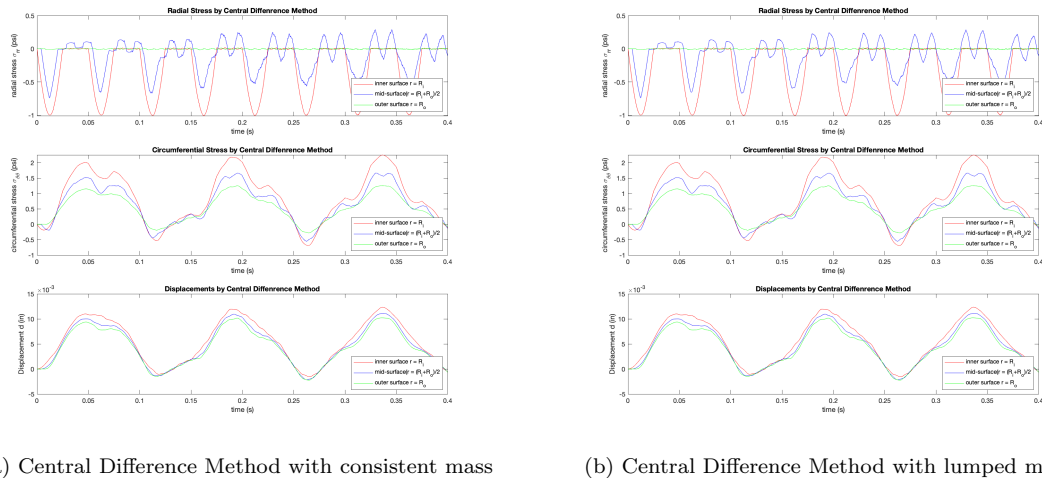


Figure 10: Numerical results by Central Difference Method with lumped or consistent mass when $\Delta t = 10^{-5}$ sec, $n_{ele} = 81$.

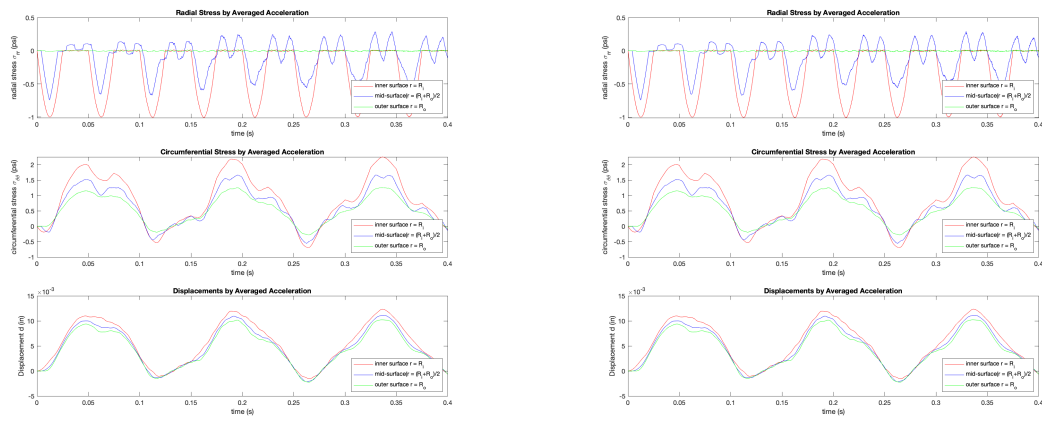


Figure 11: Numerical results by Averaged Acceleration Method with lumped or consistent mass when $\Delta t = 10^{-5}$ sec, $n_{ele} = 81$.

And we can obtain the time cycle \bar{T} in each method combination:

Table 2: \bar{T} in each method combination

	consistent mass	lumped mass
Central Difference Method	$T = 0.0499 \text{ sec}$	$T = 0.0507 \text{ sec}$
Averaged Acceleration Method	$T = 0.0505 \text{ sec}$	$T = 0.05094 \text{ sec}$

Then we can have the same observation as expected,

- Averaged Acceleration Method (Trapezoidal rule) tends to increase \bar{T} ;
- Central Difference Method tends to decrease \bar{T} ;
- lumped mass tends to increase \bar{T} ;
- consistent mass tends to decrease \bar{T} ;

Hence it was good choices to combine central difference method with lumped mass and averaged acceleration with consistent mass to neutralize the effect to the time period.